

## ANALYSIS OF FRACTIONAL ELECTRICAL CIRCUIT CONTAINING TWO RC LADDER ELEMENTS OF DIFFERENT FRACTIONAL ORDERS

Ewa PIOTROWSKA\*<sup>ORCID</sup>, Rafał MELNIK\*<sup>ORCID</sup>

\*Faculty of Computer Science and Technology, Department of Automation and Robotics,  
University of Łomża, Akademicka 1, 18-400 Łomża, Poland

[epiotrowska@al.edu.pl](mailto:epiotrowska@al.edu.pl), [rmelnik@al.edu.pl](mailto:rmelnik@al.edu.pl)

*received 20 April 2023, revised 12 June 2023, accepted 7 July 2023*

**Abstract:** The study addresses the topic of different fractional orders in the context of simulation as well as experiments using real electrical elements of fractional-order circuit. In studying the two solutions of the resistance-capacitance (RC) ladder circuit of appropriate parameters, different fractional orders of the electrical circuit are considered. Two fractional-order (non-integer) elements were designed based on the Continued Fraction Expansion (CFE) approximation method. The CFE method itself was modified to allow free choice of centre pulsation. It was also proposed that when making individual ladder circuits, in the absence of elements with the parameters specified by the program, they should be obtained by connecting commercially available elements in series or parallel. Finally, the theoretical analysis of such a circuit is presented using state-space method and verified experimentally.

**Key words:** fractional-order circuit, RC ladder, Continued Fraction Expansion

### 1. INTRODUCTION

Fractional calculus is a generalisation of classical calculus where the order can be a real or complex number. For integer orders, classical derivative is obtained. Fractional calculus has been gaining significant interest in the field of dynamical systems due to its potential for the development of mathematical models that reflect various phenomena, in the field of science and engineering [6], with higher fidelity than the models based on classical differential calculus. Moreover, its vital feature is the capability to describe the memory effect in the system [8]. For instance, the improved models of the RC, RL and RLC electrical circuits as well as supercapacitors and batteries have been successfully developed using fractional calculus [6, 9, 21].

The RC ladder network is a form of realisation of elements described as a fractional derivative, which can be used for modelling, e.g. supercapacitors or transmission lines [8, 14]. The ladder circuit is characterised by an electrical circuit configured based on series and parallel connections. Unlike supercapacitors, ladder elements have a fixed pseudocapacitance and the order of derivative has no nonlinear effects. The theory predicts that a ladder system can behave in a way that is analogous to the behaviour of fractional-order elements only if it has infinitely many components. In practice, this number is finite, which is associated with a limited use of this system as an element of the fractional order. The main problem in using a ladder circuit is the equivalent resistance, which can be derived by successively applying the series and parallel reduction formulae using the appropriate approximation. For this reason, the choice of resistance and capacitance is important. In addition, the designed ladder network should behave with the greatest possible accuracy and in a wide frequency range as an element of a fractional derivative [14, 23, 24, 26].

An example is the paper by Petras et al. [16] that proposes a relatively simple way of selecting resistance and capacitance, requiring, however, the use of a large number of passive components. In order to achieve phase compatibility (over three decades), the authors built a ladder network consisting of up to 130 meshes. The method they propose is limited to an order of 0.5.

There are other, more sophisticated, methods of selecting parameters of components such as resistance and capacitance ladder circuit in order to obtain the desired frequency range in which the ladder acts with good accuracy as a fractional with a much smaller mesh. These methods are based on the approximation of the function ( $s$  to the power of  $\alpha$ ) by the ratios of polynomials of the same degree, which also allows the selection of the required order of the derivative [5, 19, 20, 23].

Although fractional calculus was first used in 1695 by Leibniz and L'Hospital, the theory and applications of fractional calculus developed greatly in the 19th and 20th centuries, and many authors gave different definitions of fraction derivatives and integrals. Subsequently, many general calculus solutions have been developed, for example, the Riemann-Liouville fractional derivative definition, the Grünwald-Letnikov derivative definition and the Caputo fractional derivative definition [2, 3, 4, 7, 15, 22, 25, 26].

The present study is one of the first to address the topic of different fractional orders in the context of simulation as well as experiments using real elements of fractional-order RC circuit. An attempt was made to implement RC ladder networks based on Continued Fraction Expansion (CFE) development using Caputo's fractional derivative definition. For the purpose of the project, an algorithm was developed to select the parameters of passive elements included in the ladder circuits acting as physical elements of incomplete orders. Two ladder circuits of fractional orders of 0.5 and 0.7 were made. Subsequently, an electrical circuit was assembled that included both incomplete-order elements and

resistors and then tested in the time and frequency domain. Theoretical predictions were compared with the experimental data.

**2. MATHEMATICAL PRELIMINARIES**

Definition 1. The Caputo derivative of the fractional order  $\alpha \in (0, 1)$  of differentiable function  $f(t)$  is defined by Eq. (1):

$$D_t^\alpha f(t) = \frac{1}{\Gamma(1-\alpha)} \int_0^t (t-\tau)^{-\alpha} \dot{f}(\tau) d\tau \tag{1}$$

where  $\Gamma(x)$  is the Euler gamma function.

The one-sided Laplace transform of the fractional operator (Eq. [1]) is given by the following expression (Eq. [2]):

$$L[D_t^\alpha f(t)] = s^\alpha F(s) - s^{\alpha-1} f(0) \tag{2}$$

where  $F(s) = L[f(t)]$ .

Let us consider a fractional electrical element in which the current  $i(t)$  and voltage  $u(t)$  relation is described by Eq. (3):

$$i(t) = C_\alpha D_t^\alpha u(t) \tag{3}$$

where  $C_\alpha$  is called a pseudocapacitance and  $0 < \alpha \leq 1$  is the order of the element.

The impedance in  $s$ -domain of this element is represented by Eq. (4):

$$Z(s) = \frac{U(s)}{I(s)} = \frac{1}{C_\alpha s^\alpha} \tag{4}$$

and the spectral impedance is given by Eq. (5):

$$Z(j\omega) = \frac{1}{C_\alpha j^\alpha \omega^\alpha} = \frac{1}{C_\alpha [\cos(\frac{\pi\alpha}{2}) + j \sin(\frac{\pi\alpha}{2})] \omega^\alpha} \tag{5}$$

Computing the magnitude of the spectral impedance (Eq. [5]) yields the following expression (Eq. [6]):

$$A(\omega) = |Z(j\omega)| = \frac{1}{C_\alpha \omega^\alpha} \tag{6}$$

and in the logarithmic scale, we obtain the following (Eq. [7]):

$$M(\omega) = 20 \log A(\omega) = -20\alpha \log \omega - 20 \log C_\alpha \tag{7}$$

while the phase shift has the following form (Eq. [8]):

$$\varphi(\omega) = \arg Z(j\omega) = -\frac{\pi}{2} \alpha \tag{8}$$

**3. FRACTIONAL-ORDER ELECTRIC ELEMENT**

There are many different methods reported in the literature for designing electrical components of a fractional order [1, 10, 11, 17, 18, 23]. They require the selection of a certain type of electrical circuit consisting of passive elements and determining the method of selecting their parameters. A commonly used approach is to choose a circuit in the form of a ladder network consisting of  $n$  capacitors and  $n+1$  resistors, as depicted in Fig. 1.

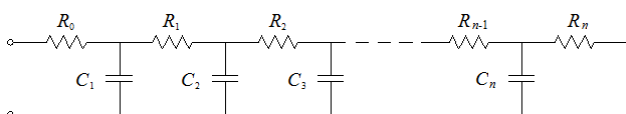


Fig. 1. Internal structure of the fractional-order element

The method of selecting parameters of an RC ladder model implementing the element described by a fractional derivative of the parameter  $\alpha$  is based on the development of the CFE [12, 13, 19, 23], as expressed by Eq. (9).

$$(1+x)^{-\alpha} = 1 - \frac{\alpha x}{1 + \frac{(1+\alpha)x}{2 + \frac{(2+\alpha)x}{3 + \frac{(2-\alpha)x}{2 + \frac{(3+\alpha)x}{2 + \frac{(3-\alpha)x}{7 + \frac{(4+\alpha)x}{2 + \dots}}}}}}}} \tag{9}$$

Due to the finite number of elements of the ladder network, amounting to  $2n + 1$ , the expansion of Eq. (9) should be finished at a certain step, allowing approximation of the  $n$ -th order of  $(1+x)^{-\alpha}$ , as presented in Eq. (10).

$$A_n^\alpha(x) = 1 - \frac{\alpha x}{1 + \frac{(1+\alpha)x}{2 + \dots + \frac{(n-1+\alpha)x}{2n-1 + \frac{(n+\alpha)x}{2}}}} \tag{10}$$

Substituting  $x = \frac{s}{\omega_0} - 1$  within Eq. (10), where  $\omega_0$  is the centre frequency, yields the following function (Eq. [11]):

$$a_n^\alpha(s) = A_n^\alpha \left( \frac{s}{\omega_0} - 1 \right) \tag{11}$$

while the approximating expression is:

$$(1+x)^{-\alpha} = \omega_0^\alpha s^{-\alpha} \tag{12}$$

This is a modification of the commonly used method that assumes  $\omega_0 = 1$  rad/s. The approximation of Eq. (11) is accurate when  $s = \omega_0$  is substituted, as indicated in Eq. (13):

$$a_n^\alpha(\omega_0) = A_n^\alpha \left( \frac{\omega_0}{\omega_0} - 1 \right) = A_n^\alpha(0) = 1 \tag{13}$$

The simplification of the continued fraction (Eq. [11]) provides the rational function of the variable  $s$  (Eq. [14]):

$$a_n^\alpha(s) = \frac{l_n s^n + l_{n-1} s^{n-1} + \dots + l_1 s + l_0}{m_n s^n + m_{n-1} s^{n-1} + \dots + m_1 s + m_0} \tag{14}$$

Implementation of the fractional element with an impedance operator as in Eq. (3) is possible based on the approximation (Eq. [14]) that yields the following expression (Eq. [15]):

$$Z(s) = \frac{\omega_0^\alpha s^{-\alpha}}{C_\alpha \omega_0^\alpha} \approx K \frac{l_n s^n + l_{n-1} s^{n-1} + \dots + l_1 s + l_0}{m_n s^n + m_{n-1} s^{n-1} + \dots + m_1 s + m_0} \tag{15}$$

Constant  $K$  is as defined in Eq. (16):

$$K = \frac{1}{C_\alpha \omega_0^\alpha} \tag{16}$$

It is a scaling constant expressed in Ohms, allowing the selection of resistance and capacitance in such a way that the currents flowing into the electrical circuit have an appropriate order of magnitude.

The diagram of the RC ladder network depicted in Fig. 1 has an impedance operator that can be expressed in terms of the following (Eq. [17]):

$$Z_n(s) = R_0 + \frac{1}{C_1 s + \frac{1}{R_1 + \frac{1}{C_2 s + \frac{1}{R_2 + \dots + \frac{1}{C_n s + \frac{1}{R_n}}}}}} \tag{17}$$

The results that we obtain by developing a rational function  $Z_n(s)$  in a continued fraction with individual resistances  $R_k$  and capacitances  $C_k$  would be as in Eq. (17).

The above procedure makes it possible to design a ladder network of fractional order  $\alpha$  based on the scaling constant  $K$ , the center pulsation  $\omega_0$  and the number of capacitors  $n$ . The algorithm consists of the following steps:

1. Input of a set of ladder network parameters:
  - a. order of derivative  $\alpha$ ,
  - b. number of capacitors  $n$ ,
  - c. scaling constant  $K$ ,
  - d. centre pulsation  $\omega_0$ .
2. Calculation of coefficients  $l_k$  and  $m_k$  of polynomials being the numerator and denominator of the right side of Eq. (15).
3. Determination of the coefficients  $R_k$  and  $C_k$  of the expansion provided in Eq. (17), based on knowledge of  $l_k$  and  $m_k$  and the constant  $K$ .

**4. USING THE TEMPLATE RC LADDER MODEL BASED ON CFE DEVELOPMENT**

The CFE method was used to design an RC ladder circuit according to the diagram in Fig. 1. Adoption of the assumed input parameters was as the following: order of the derivative  $\alpha_1 = 0.5$ , constant  $K_1 = 2087.67 \Omega$ , centre frequency  $f_0 = 100$  Hz and the number of meshes of the ladder network  $n = 30$ ; this allowed the procurement of parameters of the RC ladder network elements predicted by the program: resistance values of the resistors and capacitances values of the capacitors.

Due to the limited availability of the elements with the desired parameters on the market and discrepancies between the values declared by the manufacturer and the measured ones, the resulting resistances and capacitances provided by the program had to be obtained by building equivalent systems. In most cases, it was sufficient to select pairs of elements, which were then connected in series or parallel. To this end, the program was developed for selecting equivalent resistances and capacitances as well as an appropriate way of combining them – so as to obtain the value as close as possible to that anticipated by the program. This procedure allowed parameters to be selected with an error of less than 1%. Tabs. 1 and 2 summarise the parameters for the ladder network of  $\alpha_1 = 0.5$ . The second and third columns contain the measured values of resistive elements (Tab. 1) and capacitances (Tab. 2) used to build the ladder network. The fourth column shows connection of the elements. The fifth column contains the parameters of the equivalent systems, while the sixth column contains the parameters determined by the algorithm. The software used for the calculations (and plotting) was Wolfram Mathematica 9.0.

MLCC ceramic capacitors were used to build the ladder circuit model. Resistance and capacitance measurements were made with the LCR meter by HM8118 Rohde & Schwarz at 120 Hz.

Similar to the present method, a row RC ladder network of an order  $\alpha_2 = 0.7$  was designed. For the purpose of the algorithm, the following assumptions were made: scaling constant  $K_2 = 1010 \Omega$ , centre frequency  $f_0 = 100$  Hz and number of capacitors  $n = 30$ .

**Tab. 1.** Equivalent capacitances and their connection

No.	$C_a$	$C_b$	Connection	$C_{ab}$	$C$
1	34.08 nF	3.42 nF	Parallel	37.5 nF	37.5 nF
2	10.2 $\mu$ F	88.4 nF	Series	87.6 nF	87.6 nF
3	137 nF	1.43 nF	Parallel	138 nF	138 nF
4	99.4 nF	89.4 nF	Parallel	189 nF	189 nF
5	945 nF	322 nF	Series	240 nF	240 nF
6	225 nF	67.3 nF	Parallel	293 nF	293 nF
7	346 nF	-	None	346 nF	346 nF
8	337 nF	63.3 nF	Parallel	401 nF	401 nF
9	1.51 $\mu$ F	654 nF	Series	457 nF	457 nF
10	474 nF	40.6 nF	Parallel	514 nF	514 nF
11	348 nF	226 nF	Parallel	574 nF	574 nF
12	637 nF	-	None	637 nF	636 nF
13	661 nF	40.1 nF	Parallel	702 nF	702 nF
14	1.54 $\mu$ F	1.54 $\mu$ F	Series	770 nF	770 nF
15	633 nF	210 nF	Parallel	843 nF	842 $\mu$ F
16	10.1 $\mu$ F	1.01 $\mu$ F	Series	920 nF	919 nF
17	983 nF	19.3 nF	Parallel	1.00 $\mu$ F	1.00 $\mu$ F
18	675 nF	416 nF	Parallel	1.09 $\mu$ F	1.09 $\mu$ F
19	975 nF	212 nF	Parallel	1.19 $\mu$ F	1.19 $\mu$ F
20	663 nF	632 nF	Parallel	1.30 $\mu$ F	1.30 $\mu$ F
21	954 nF	458 nF	Parallel	1.41 $\mu$ F	1.42 $\mu$ F
22	1.50 $\mu$ F	46.7 nF	Parallel	1.55 $\mu$ F	1.55 $\mu$ F
23	1.02 $\mu$ F	685 nF	Parallel	1.71 $\mu$ F	1.71 $\mu$ F
24	1.55 $\mu$ F	348 nF	Parallel	1.89 $\mu$ F	1.89 $\mu$ F
25	1.49 $\mu$ F	629 nF	Parallel	2.12 $\mu$ F	2.12 $\mu$ F
26	1.49 $\mu$ F	909 nF	Parallel	2.40 $\mu$ F	2.40 $\mu$ F
27	719 nF	1.03 $\mu$ F	Parallel	2.78 $\mu$ F	2.78 $\mu$ F
28	10.6 $\mu$ F	4.88 $\mu$ F	Parallel	3.34 $\mu$ F	3.34 $\mu$ F
29	434 nF	2.28 $\mu$ F	Parallel	4.29 $\mu$ F	4.28 $\mu$ F
30	5.15 $\mu$ F	1.45 $\mu$ F	Parallel	6.60 $\mu$ F	6.59 $\mu$ F

**Tab. 2.** Equivalent resistances and their connection

No.	$R_a$	$R_b$	Connection	$R_{ab}$	$R$
0	739 $\Omega$	35.9 $\Omega$	Parallel	34.2 $\Omega$	34.2 $\Omega$
1	802 $\Omega$	218 $\Omega$	Parallel	171 $\Omega$	171 $\Omega$
2	5.07 k $\Omega$	329 $\Omega$	Parallel	309 $\Omega$	309 $\Omega$
3	2.35 k $\Omega$	553 $\Omega$	Parallel	447 $\Omega$	447 $\Omega$
4	555 $\Omega$	32.8 $\Omega$	Series	587 $\Omega$	588 $\Omega$
5	662 $\Omega$	67.2 $\Omega$	Series	730 $\Omega$	729 $\Omega$
6	612 $\Omega$	262 $\Omega$	Series	874 $\Omega$	874 $\Omega$
7	2.14 k $\Omega$	1.96 k $\Omega$	Parallel	1.02 k $\Omega$	1.02 k $\Omega$
8	272 k $\Omega$	1.18 k $\Omega$	Parallel	1.17 k $\Omega$	1.17 k $\Omega$
9	12.9 k $\Omega$	1.48 k $\Omega$	Parallel	1.33 k $\Omega$	1.33 k $\Omega$
10	9.80 k $\Omega$	1.76 k $\Omega$	Parallel	1.49 k $\Omega$	1.49 k $\Omega$
11	5.54 k $\Omega$	2.36 k $\Omega$	Parallel	1.66 k $\Omega$	1.66 k $\Omega$
12	4.19 k $\Omega$	3.26 k $\Omega$	Parallel	1.83 k $\Omega$	1.83 k $\Omega$
13	1.96 k $\Omega$	55.0 $\Omega$	Series	2.01 k $\Omega$	2.01 k $\Omega$
14	13.0 k $\Omega$	2.66 k $\Omega$	Parallel	2.21 k $\Omega$	2.21 k $\Omega$
15	2.36 k $\Omega$	50.4 $\Omega$	Series	2.41 k $\Omega$	2.41 k $\Omega$
16	8.05 k $\Omega$	3.90 k $\Omega$	Parallel	2.63 k $\Omega$	2.63 k $\Omega$
17	1.77 k $\Omega$	1.10 k $\Omega$	Series	2.86 k $\Omega$	2.86 k $\Omega$
18	2.92 k $\Omega$	195 $\Omega$	Series	3.12 k $\Omega$	3.12 k $\Omega$
19	17.7 k $\Omega$	4.21 k $\Omega$	Parallel	3.40 k $\Omega$	3.40 k $\Omega$
20	30.1 k $\Omega$	4.23 k $\Omega$	Parallel	3.71 k $\Omega$	3.71 k $\Omega$
21	3.84 k $\Omega$	215 $\Omega$	Series	4.06 k $\Omega$	4.05 k $\Omega$
22	38.5 k $\Omega$	5.04 k $\Omega$	Parallel	4.45 k $\Omega$	4.45 k $\Omega$
23	2.95 k $\Omega$	1.97 k $\Omega$	Series	4.92 k $\Omega$	4.92 k $\Omega$
24	240 k $\Omega$	5.60 k $\Omega$	Parallel	5.47 k $\Omega$	5.47 k $\Omega$
25	26.4 k $\Omega$	8.03 k $\Omega$	Parallel	6.16 k $\Omega$	6.16 k $\Omega$
26	6.82 k $\Omega$	235 $\Omega$	Series	7.05 k $\Omega$	7.05 k $\Omega$
27	55.4 k $\Omega$	9.76 k $\Omega$	Parallel	8.29 k $\Omega$	8.29 k $\Omega$
28	8.95 k $\Omega$	1.29 k $\Omega$	Series	10.2 k $\Omega$	10.2 k $\Omega$
29	29.89 k $\Omega$	26.4 k $\Omega$	Parallel	14.0 k $\Omega$	14.0 k $\Omega$
30	738 k $\Omega$	29.9 k $\Omega$	Parallel	28.7 k $\Omega$	28.7 k $\Omega$

### 5. FREQUENCY RESPONSE OF THE LADDER CIRCUIT MODEL

Due to the complexity of the ladder networks and the number of their elements, Bode plots of incomplete systems, spanning four decades (1–10 kHz), were investigated. Figs. 2 and 3 present the amplitude and phase characteristics for an RC ladder model of an order  $\alpha_1 = 0.5$  and pseudocapacitance  $C_{\alpha_1} = 19.1 \mu\text{F/s}^{0.5}$ .

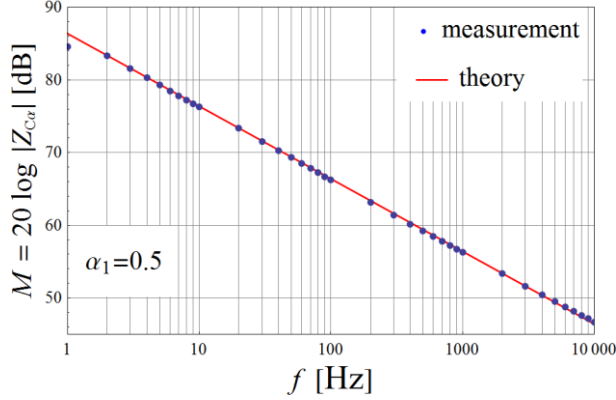


Fig. 2. Bode magnitude plot for the RC ladder circuit of an order  $\alpha_1 = 0.5$

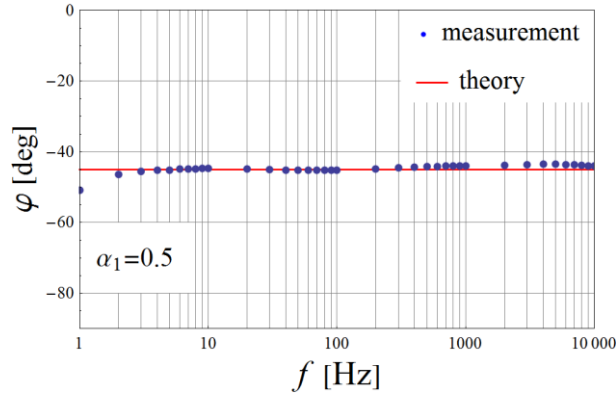


Fig. 3. Bode phase plot for the RC ladder circuit of an order  $\alpha_1 = 0.5$

In turn, Figs. 4 and 5 depict the frequency responses of the ladder network of an incomplete order  $\alpha_2 = 0.7$  and pseudocapacitance  $C_{\alpha_2} = 10.9 \mu\text{F/s}^{0.5}$ .

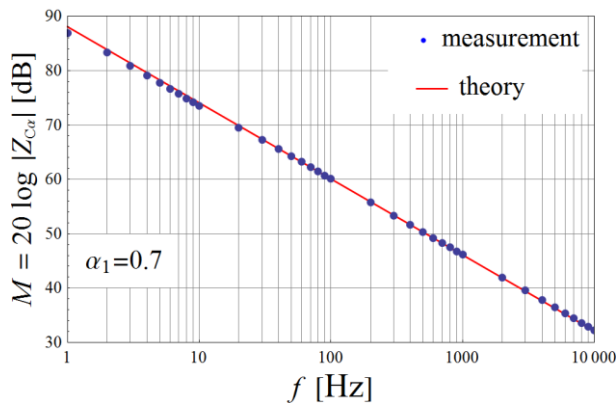


Fig. 4. Bode magnitude plot for the RC ladder circuit of an order of  $\alpha_2 = 0.7$

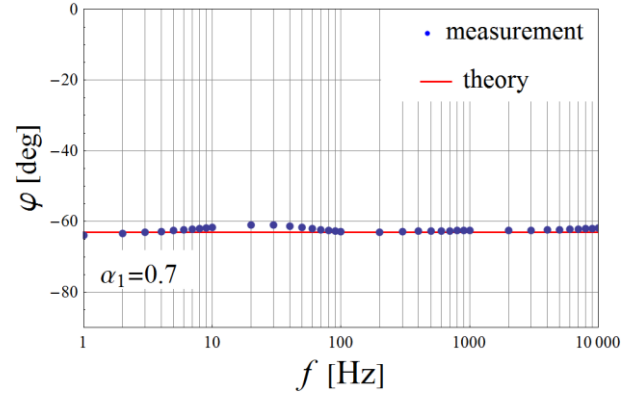


Fig. 5. Bode phase plot for the RC ladder circuit of an order of  $\alpha_2 = 0.7$

The obtained phase characteristics for the RC ladder with an order of 0.5 deviate from the theoretical value ( $-45^\circ$ ) by no more than  $1.5^\circ$ . In contrast, the measured magnitude deviates from the theoretical line by less than 0.7%. The measured phase characteristic for the RC ladder of a fractional order of  $\alpha_2 = 0.7$  deviates from the theoretical value ( $-63^\circ$ ) by no more than  $2.2^\circ$ . The Bode magnitude plot for the system of  $\alpha_2$ , based on the measurement, is consistent with the theoretical response, differing less than 0.8%.

### 6. ELECTRICAL FRACTIONAL CIRCUIT

The diagram of the measuring system, shown in Fig. 6, consists of three external resistors  $R_1$ ,  $R_2$  and  $R_3$ , constant voltage source  $e$  and two elements of orders  $\alpha_1$  and  $\alpha_2$ .

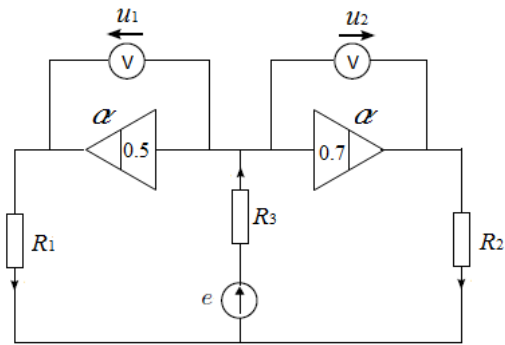


Fig. 6. Diagram of the RC electrical circuit

The dynamics of the voltages at the terminals of both ladder circuits are given by the state-space representation (Eq. [18]):

$$\begin{bmatrix} D_t^{\alpha_1} u_1(t) \\ D_t^{\alpha_2} u_2(t) \end{bmatrix} = \begin{bmatrix} a_{11} & a_{12} \\ a_{21} & a_{22} \end{bmatrix} \begin{bmatrix} u_1(t) \\ u_2(t) \end{bmatrix} + \begin{bmatrix} b_1 \\ b_2 \end{bmatrix} e(t) \quad (18)$$

where:

$$A = \begin{bmatrix} a_{11} & a_{12} \\ a_{21} & a_{22} \end{bmatrix} = \begin{bmatrix} -\frac{R_2+R_3}{R^2 C_{\alpha_1}} & \frac{R_3}{R^2 C_{\alpha_1}} \\ \frac{R_3}{R^2 C_{\alpha_2}} & -\frac{R_1+R_3}{R^2 C_{\alpha_2}} \end{bmatrix} \quad (19a)$$

$$B = \begin{bmatrix} b_1 \\ b_2 \end{bmatrix} = \begin{bmatrix} \frac{R_2}{R^2 C_{\alpha_1}} \\ \frac{R_1}{R^2 C_{\alpha_2}} \end{bmatrix} \quad (19b)$$

$$R^2 = R_1 R_2 + R_2 R_3 + R_1 R_3 \quad (19c)$$

The solution of the equation of state (Eq. [20]) is as follows:

$$x(t) = \Phi_0(t)x_0 + \int_0^t [\Phi_1(t-\tau)\tilde{B}_1 + \Phi_2(t-\tau)\tilde{B}_2]e(\tau)d\tau \quad (20)$$

where  $x(t) = \begin{bmatrix} u_1(t) \\ u_2(t) \end{bmatrix}$  is a state vector with  $x_0 = x(0)$ , while

$$\tilde{B}_1 = \begin{bmatrix} b_1 \\ 0 \end{bmatrix}, \tilde{B}_2 = \begin{bmatrix} 0 \\ b_2 \end{bmatrix} \quad (21)$$

Time-dependent functions  $\Phi_k(t)$  for  $k = 0,1,2$ , occurring in the solution of Eq. (19), are given by functional series, as presented in Eq. (22):

$$\begin{aligned} \Phi_0(t) &= \sum_{k_1=0}^{\infty} \sum_{k_2=0}^{\infty} T_{k_1 k_2} \frac{t^{k_1 \alpha_1 + k_2 \alpha_2}}{\Gamma(k_1 \alpha_1 + k_2 \alpha_2 + 1)} \\ \Phi_1(t) &= \sum_{k_1=0}^{\infty} \sum_{k_2=0}^{\infty} T_{k_1 k_2} \frac{t^{(k_1+1)\alpha_1 + k_2 \alpha_2 - 1}}{\Gamma[(k_1+1)\alpha_1 + k_2 \alpha_2]} \\ \Phi_2(t) &= \sum_{k_1=0}^{\infty} \sum_{k_2=0}^{\infty} T_{k_1 k_2} \frac{t^{k_1 \alpha_1 + (k_2+1)\alpha_2 - 1}}{\Gamma[k_1 \alpha_1 + (k_2+1)\alpha_2]} \end{aligned} \quad (22)$$

where data in the form of matrices  $T_{k_1 k_2}$  are provided in terms of the following recursive relationship (Eq. [23]):

$$f(x) = \begin{cases} I_N & \text{for } k_1 = k_2 = 0 \\ \tilde{A}_1 T_{k_1-1, k_2} + \tilde{A}_2 T_{k_1, k_2-1} & \text{for } k_1, k_2 \geq 0 \\ & \text{and } k_1 = k_2 = 0 \\ 0 & \text{for } k_1 < 0 \\ & \text{and/or } k_2 < 0 \end{cases} \quad (23)$$

where

$$\tilde{A}_1 = \begin{bmatrix} a_{11} & a_{12} \\ 0 & 0 \end{bmatrix}, \tilde{A}_2 = \begin{bmatrix} 0 & 0 \\ a_{21} & a_{22} \end{bmatrix} \quad (24)$$

## 7. MEASUREMENTS OF THE ELECTRICAL CIRCUIT

The RC ladder network of fractional orders  $\alpha_1 = 0.5$  and  $\alpha_2 = 0.7$  was assembled (Fig. 7) according to the scheme presented in Fig. 6. The values of the parameters of the circuit elements are presented in Tab. 3.

Tab. 3. Parameters of the circuit

Circuit parameters	Values
$R_1$	996.8 $\Omega$
$R_2$	1183.0 $\Omega$
$R_3$	893.8 $\Omega$
$\alpha_1$	0.5
$\alpha_2$	0.7
$C_{\alpha_1}$	19.1 $\mu\text{F}/\text{s}^{0.5}$
$C_{\alpha_2}$	10.9 $\mu\text{F}/\text{s}^{0.3}$
$e$	10 V

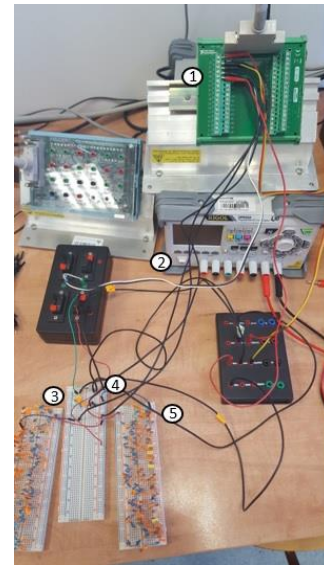


Fig. 7. Measuring station used in the experiment: 1 – measuring card; 2 – DC power supply; 3 – ladder network of  $\alpha_1 = 0.5$ ; 4 – boards with external resistors; 5 – ladder network of  $\alpha_2 = 0.7$

The RC ladder network and DC voltage terminals were connected to the measuring card. The discharged circuit was fed with a step voltage of 10 V. During the experiment, the dynamics of terminal voltage of the ladder circuits with a time step of 1 ms were measured.

Figs. 8 and 9 present the step responses of the fractional-order RC circuit; further, Tab. 3 presents theoretical curves based on Eq. (19) and parameters of the tested circuit elements.

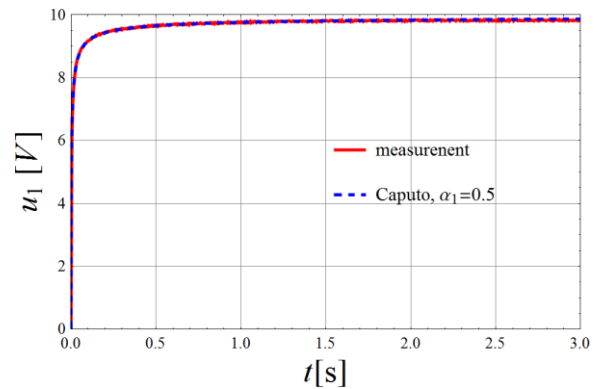


Fig. 8. Measured and theoretical step response of the RC ladder circuit of  $\alpha_1 = 0.5$

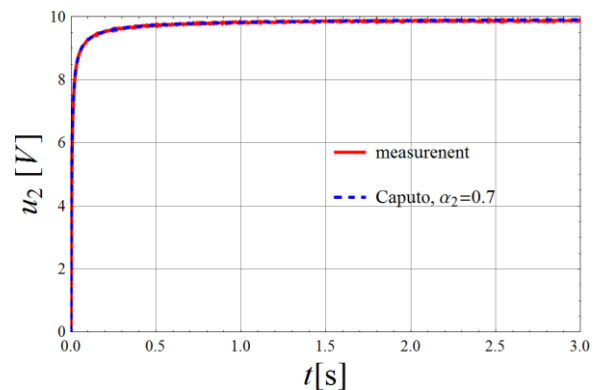


Fig. 9. Measured and theoretical step response of the RC ladder circuit of  $\alpha_2 = 0.7$

The accuracy of the results is analysed through a comparison of theoretical and measured values of both curves using relative error (Eq. [25]):

$$\varepsilon = \left| \frac{u_{\text{theoretical}} - u_{\text{measured}}}{u_{\text{measured}}} \right| \cdot 100\% \quad (25)$$

The relative error curves are presented in Figs. 10 and 11.

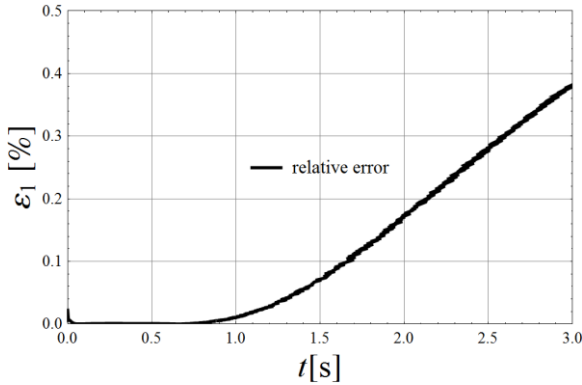


Fig. 10. Relative error function of the RC ladder circuit of  $\alpha_1 = 0.5$

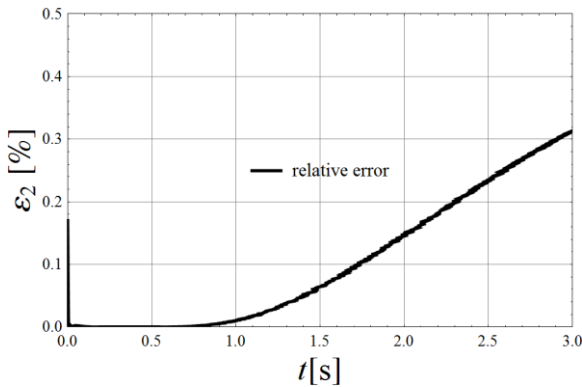


Fig. 11. Relative error function of the RC ladder circuit of  $\alpha_2 = 0.7$

The relative error in both the cases did not exceed 0.5%.

## 8. CONCLUSIONS

Realisation methods of an RC ladder circuit of fractional order, associated with the appropriate selection of its resistance and capacitance, were discussed. Previous approaches described by Khazali and Tawalbeh [5], as well as Petras, Sierociuk and Podlubny [16], have significant restrictions as to the choice of order of derivative  $\alpha$ . Despite their simplicity, consisting in a small variation of the parameters of the selected elements, the above methods require the construction of systems of considerable length in order to obtain a wide frequency range in which RC ladder behaves in a manner as close as possible to the ideal element of the order  $\alpha_1 = 0.5$ .

For this reason, the paper considers the case when  $\alpha$  is different from 0.5 (in this case  $\alpha = 0.7$ ) and compares the obtained results with the results of  $\alpha = 0.5$ . In this way, the description and development of the ladder electrical circuits with  $\alpha$  other than 0.5 were presented, thereby enabling a wider application of fractional differential calculus. An approximation based on CFE was used, which made it possible to shorten the ladder calculations of elec-

trical circuits. The definition of fractional order by Caputo was also used.

In order to obtain the values of the resistance and capacitance of the RC ladder network, consistent with the theoretical values calculated based on CFE, a program was developed that selects the equivalent, actual resistors and capacitors with the measured values and the way of their connection. As a result, the discrepancy between the actual and theoretical values was at most 1%.

In this way, the circuits consisting of fewer meshes and having a wider range of Bode plot compatibility were obtained and compared with the results derived by the aforementioned authors. The study also shows that for the circuit comprising two real fractional elements, the theoretical predictions do not differ from the experimental results by more than 0.5% of the measured value.

## REFERENCES

1. Alsaedi A, Nieto JJ, Venkatesh V. Fractional electrical circuits. *Advances in Mechanical Engineering*. 2015 Dec 1; 7 (12): 168781401561812.
2. Al-Refai M, Abdeljawad T. Analysis of the fractional diffusion equations with fractional derivative of non-singular kernel. *Adv Differ Equ*. 2017; (1): 315.
3. M. Batiha I, A. Njadat S, M. Batiha R, Zraiqat A, Dababneh A, Momani S. Design Fractional-order PID Controllers for Single-Joint Robot Arm Model. *ijasca*. 2022 Aug 1; 14 (2): 97–114.
4. Chen W, HongGuang S, Xicheng L. *Fractional Derivative Modeling in Mechanics and Engineering*. 1st ed. Springer; 2022. 385 p.
5. El-Khazali R, Tawalbeh N. Realization of Fractional-Order Capacitors and Inductors. In: *Proceedings of The 5th Workshop on Fractional Differentiation and its Applications*. Hohai University, Nanjing, China; 2012; 1–6.
6. Correa-Escudero IL, Gómez-Aguilar JF, López-López MG, Alvarado-Martínez VM, Baleanu D. Correcting dimensional mismatch in fractional models with power, exponential and proportional kernel: Application to electrical systems. *Results in Physics*. 2022 Sep; 40:105867.
7. Evangelista LR, Lenzi EK. *An introduction to anomalous diffusion and relaxation*. Cham, Switzerland: Springer Nature; 2023. 400 p.
8. Hidalgo-Reyes JI, Gómez-Aguilar JF, Escobar-Jiménez RF, Alvarado-Martínez VM, López-López MG. Classical and fractional-order modeling of equivalent electrical circuits for supercapacitors and batteries, energy management strategies for hybrid systems and methods for the state of charge estimation: A state of the art review. *Microelectronics Journal*. 2019 Mar; 85:109–28.
9. Hidalgo-Reyes JI, Gómez-Aguilar JF, Escobar-Jimenez RF, Alvarado-Martinez VM, Lopez-Lopez MG. Determination of supercapacitor parameters based on fractional differential equations. *Int J Circ Theor Appl*. 2019 May 22; cta.2640.
10. Kaczorek T. Analysis of Fractional Electrical Circuits in Transient States. In *Logitrans - VII Konferencja Naukowo-Techniczna*; 2010; 1695–704.
11. Kaczorek T, Rogowski K. *Fractional Linear Systems and Electrical Circuits*. Springer International Publishing; 2015. (Studies in Systems, Decision and Control; vol. 13). <https://link.springer.com/10.1007/978-3-319-11361-6>
12. Krishna BT, Reddy KVVS. Active and Passive Realization of Fractional Device of Order 1/2. *Active and Passive Electronic Components*. 2008;2008:1–5.
13. Kumar N, Upadhyay DK. Fractional Order Digital Differentiator with Linear Phase and Low Absolute Error. *International Journal of Electronic and Electrical Engineering*. 2014;7(5):491–6.
14. Mitkowski W, Bauer W, Zagórska M. RC-ladder networks with supercapacitors. *Archives of Electrical Engineering*. 2018; 67 (2): 377–89.

15. Mitkowski W, Długosz M, Skruch P. Selected Engineering Applications of Fractional-Order Calculus. In: Kulczycki P, Korbicz J, Kacprzyk J, editors. Fractional Dynamical Systems: Methods, Algorithms and Applications [Internet]. Cham: Springer International Publishing; 2022 [cited 2023 Sep 7]. p. 333–59. (Studies in Systems, Decision and Control; vol. 402). Available from: [https://link.springer.com/10.1007/978-3-030-89972-1\\_12](https://link.springer.com/10.1007/978-3-030-89972-1_12)
16. Petras I, Sierociuk D, Podlubny I. Identification of Parameters of a Half-Order System. IEEE Trans Signal Process. 2012 Oct; 60 (10): 5561–6.
17. Piotrowska E. Analysis of fractional capacitor and coil by the use of the Conformable Fractional Derivative and Caputo definitions. In: 2018 International Interdisciplinary PhD Workshop (IIPhDW). Swinoujście: IEEE. 2018; 103–7. <https://ieeexplore.ieee.org/document/8388335/>
18. Piotrowska E, Rogowski K. Analysis of Fractional Electrical Circuit Using Caputo and Conformable Derivative Definitions. In: Ostalczyk P, Sankowski D, Nowakowski J, editors. Non-Integer Order Calculus and its Applications: Springer International Publishing; 2019, p. 183–94. (Lecture Notes in Electrical Engineering; vol. 496). [http://link.springer.com/10.1007/978-3-319-78458-8\\_16](http://link.springer.com/10.1007/978-3-319-78458-8_16)
19. Podlubny I, Petráš I, Vinagre BM, O’Leary P, Dorčák L. Analogue Realization of Fractional-Order Controlers. Nonlinear Dynamics. 2002;29(1/4):281–96.
20. Pu Yifei, Yuan Xiao, Liao Ke, Zhou Jiliu, Zhang Ni, Zeng Yi, et al. Structuring Analog Fractance Circuit for 1/2 Order Fractional Calculus. In: 2005 6th International Conference on ASIC. Shanghai, China: IEEE; 2005, 1039–42. <http://ieeexplore.ieee.org/document/1611507/>
21. Sene N, Gómez-Aguilar JF. Analytical solutions of electrical circuits considering certain generalized fractional derivatives. Eur Phys J Plus. 2019 Jun;134(6):260.
22. Sierociuk D, Skovranek T, Macias M, Podlubny I, Petras I, Dzieliński A, et al. Diffusion process modeling by using fractional-order models. Applied Mathematics and Computation. 2015; 257:2–11.
23. Sierociuk D, Dzieliński A. Ultracapacitor Modelling and Control Using Discrete Fractional Order State-Space Model. Acta Montanistica Slovaca. 2008;13(1):136–45.
24. Skovranek T, Macias M, Sierociuk D, Malesza W, Dzieliński A, Podlubny I, et al. Anomalous diffusion modeling using ultracapacitors in domino ladder circuit. Microelectronics Journal. 2019; 84:136–41.
25. Tapadar A, Khanday FA, Sen S, Adhikary A. Fractional calculus in electronic circuits: a review. In: Fractional Order Systems [Internet]. Elsevier; 2022 [cited 2023 Sep 7]. p. 441–82. Available from: <https://linkinghub.elsevier.com/retrieve/pii/B978012824293300018>
26. Yang XJ. General fractional derivatives: theory, methods and applications. Boca Raton, FL: CRC Press, Taylor & Francis Group; 2019.

Ewa Piotrowska:  <https://orcid.org/0000-0003-3163-0753>

Rafał Melnik:  <https://orcid.org/0000-0003-2900-784X>



This work is licensed under the Creative Commons BY-NC-ND 4.0 license.